

Evaluation of the water resource for four large hydropower potentials in Southwest Greenland

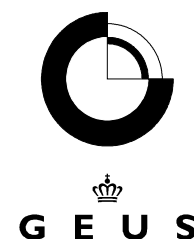
The industrial potentials 06.g, 07.d, 07.e and 07.f, and their development over the period 1980-2014

Andreas P. Ahlstrøm, Dorthe Petersen, Kenneth D. Mankoff,
Robert S. Fausto, Signe B. Andersen, Nanna B. Karlsson,
Karina Hansen, Peter L. Langen &
Ruth H. Mottram

MISISSUEQQAARNERIT/GRØNLANDS FORUNDERSØGELSER
AATSITASSANUT IKUMMATISSANULLU NAALAKKERSUISOQARFIK
DEPARTEMENTET FOR RÅSTOFFER - NAALAKKERSUISUT



DE NATIONALE GEOLOGISKE UNDERSØGELSER
FOR DANMARK OG GRØNLAND,
ENERGI-, FORSYNINGS- OG KLIMAMINISTERIET



Contents

Introduction	4
Background	5
Evolution of the water resource in Southwest Greenland	7
Four previously assessed hydropower potentials	13
Method	15
Measuring the water resource	15
Water level registration	15
Stage-discharge relation.....	16
Manual discharge measurements	16
Time series of the water resource	17
Filling of data gaps in measured time series	17
Statistical evaluation	18
Delineation of catchments	19
Error analysis of the catchment delineation	20
Model-based discharge	22
Hydropower potential 06.g	24
Monitoring of the water resource	24
Establishing the 1980-2014 time series	26
The water resource.....	27
Hydropower potential 07.d	29
Monitoring of the water resource	29
Establishing the 1980-2014 time series	30
The water resource.....	31
Hydropower potential 07.e	34
Monitoring of the water resource	34
Establishing the 1980-2014 time series	35
The water resource.....	35
Hydropower potential 07.f	38
Monitoring of the water resource	38
Establishing the 1980-2014 time series	39
The water resource.....	40
Conclusion	43
References	46

Introduction

This report is a collaborative effort between GEUS and Asiaq, requested by the Ministry of Industry, Labour, Trade and Energy, Government of Greenland in consultation with Nukis-siorfiit.

The aim is an updated evaluation of the water resources available to four large hydropower potentials in Southwest Greenland: the catchments 06.g, 07.d, 07e and 07.f. The evaluation covers the period 1980-2014 and is based on data collected by Asiaq (previously the Greenland Technical Organisation), supported by output from the regional climate model HIRHAM5 provided by the Danish Meteorological Institute, and glaciological/glacier hydrological data and methods employed by the Geological Survey of Denmark and Greenland.

Background

Hydropower is a key element in the transition of the Greenlandic energy supply towards sustainable energy. The continued expansion of the hydropower capacity in Greenland will be crucial for combining economical growth of the Greenlandic society with sustainable development. On the global scale, hydropower is growing, with an additional 31.5 GW installed worldwide in 2016, out of which hydropower serving as a reservoir for the more variable solar and wind power consisted of 6.4 GW (IHA, 2017)

The potential for hydropower in Greenland is intimately related to the amount of meltwater from the Greenland ice sheet as well as the amount of precipitation. The ongoing changes in global climate thus have immediate economical consequences for Greenland and must be taken into account when developing a strategy for the future energy supply. Climate change is accelerated in the Arctic, where the temperature is increasing nearly twice as fast as for the global mean, and the atmospheric circulation patterns appear to be shifting (AMAP, 2017). The increased contribution to sea level rise of the Greenland ice sheet is causing concern globally, but climate change is also important for the Greenlandic society on the local scale.

Climate change implies that the existing survey of the hydropower potential of Greenland presented in the Nukissiorfiit report (in Danish) "Grønlands vandkraftressourcer. En oversigt – August 2005" (Nukissiorfiit, 2005) most likely underestimates the actual present size of the hydropower potentials. Climate change also implies that the variability from year to year has become more important – this parameter was not included in the report from 2005. The hydropower potential of partially ice-covered catchments is primarily affected by changes in meltwater runoff, while for ice-free catchments it is mainly affected by changes in precipitation patterns.

The Greenland Government supports the collection of fundamental data from a range of the larger hydropower potentials, permitting the derivation of actual discharge. For obvious reasons, data from the period after 2005 is not included in the report from Nukissiorfiit from 2005. There is therefore clearly merit in carrying out an updated analysis of the hydropower potential of Greenland, exploiting available discharge measurements and the various extensive recent datasets made available from the intense research on the contribution of the Greenland ice sheet to sea level rise.

This report presents results from the second phase of an effort to update the existing survey from 2005 of the hydropower potential in Greenland from Nukissiorfiit, where the first phase was an preliminary analysis, presented in GEUS-Notat 10-NA-17-01 (Ahlstrøm and others, 2017). In this report we initially present results from this analysis for Southwest Greenland, followed by an evaluation of the four hydropower potentials of industrial interest with most documentation, named 07.d, 07.e, 07.f and 06.g and situated south of Kangerlussuaq and northeast of Nuuk and Maniitsoq, with names derived from Nukissiorfiit (2005). These catchments are dominated by meltwater runoff from the Greenland ice sheet and the delineation carried out in this analysis will be based on the current ice sheet surface. Thus, we will present no risk evaluation of catchment changes or variability due to ice sheet retreat or changes

in the internal hydrological drainage of the ice sheet. We will provide an estimate of the development of the water resource of the hydropower potentials over the period 1980-2014, based on a combination of data collected in the field and results from numerical models. Field data are available for varying durations of this period for all four catchments presented.

The four hydropower potentials evaluated in this report are all considered specifically attractive for energy intensive industries, as for example large international data centres.

Evolution of the water resource in Southwest Greenland

A first step in establishing a sufficient foundation for policy-making on the possible future development of hydropower in Greenland is to determine the impact of the climate change which has already occurred. A preliminary analysis of this change was provided in GEUS-Notat 10-NA-17-01 (Ahlstrøm and others, 2017) and we reiterate the results in the following as they provide a relevant framework for the analysis of the individual hydropower potentials. For the preliminary analysis we employed a regional climate model designed to utilize measured meteorological parameters and which provides results for the ice sheet meltwater runoff as well as the runoff from ice-free terrain driven by precipitation. This division makes it possible to obtain an overview of the industrial-size hydropower potentials primarily depending on ice sheet meltwater runoff, as well as the smaller hydropower potentials in the vicinity of populated areas which depend primarily on precipitation over the ice-free terrain. We have employed results from a model experiment with the regional climate model HIRHAM5 of the Danish Meteorological Institute (DMI) which meets the requirements stated above, and used the data over the most relevant region for hydropower in Greenland (the model domain is shown in Fig. 1).



Figure 1. Map showing the chosen model domain (red polygon) in Southwest Greenland of the regional climate model experiment with HIRHAM5.

The vast majority of Greenland's exploitable hydropower potential is situated between Ilulissat in West Greenland and Nanortalik in the far south. Accordingly, this region is chosen for further analysis of the evolution of the runoff from the ice sheet and the ice-free terrain, respectively, as estimated by the regional climate model HIRHAM5 of DMI. The model was run using so-called re-analysis data from the ERA-Interim dataset over the period 1980-2014, which implies that the numerical modelling was, as far as possible, based on observed data. The model operates on a horizontal resolution of 5.5 km, providing output every 90 seconds and is described in more detail in Ahlstrøm & Petersen and others (2017). For this analysis, we have chosen to focus on the difference in runoff between the first 12 years (1980-1991) and the last 12 years (2003-2014) of the period investigated for the ice sheet and ice-free terrain, respectively. The latter 12-year period is chosen because the region appears to have experienced an abrupt shift in climate since 2003 (Ahlstrøm & Petersen and others, 2017), whereas the first 12-year period is chosen as the earliest possible 12-year interval in the model experiment. The difference between the two 12-year periods is subsequently shown partly with a colour-coded map of Southwest Greenland and partly with a plot illustrating the difference in the monthly mean runoff from the entire model domain delineated in Fig. 1.

The result of the model experiment for ice sheet runoff is shown in Fig. 2. Here, Fig. 2a shows how the difference in runoff between the two 12-year periods is distributed geographically over an area approaching 100 km in width from the ice margin and inwards, with an annual mean difference reaching above 800 mm water equivalent (ie. the amount of water corresponding the ice melted away). Fig. 2b shows the same result, with the difference illustrated as additional runoff (in percent) going from the former 12-year period to the latter. The red colour in Fig. 2b illustrates the expansion of the area experiencing melt. At higher elevations on the ice sheet, meltwater refreezes in the underlying snow which is below the freezing point, keeping the meltwater from leaving the ice sheet as runoff.

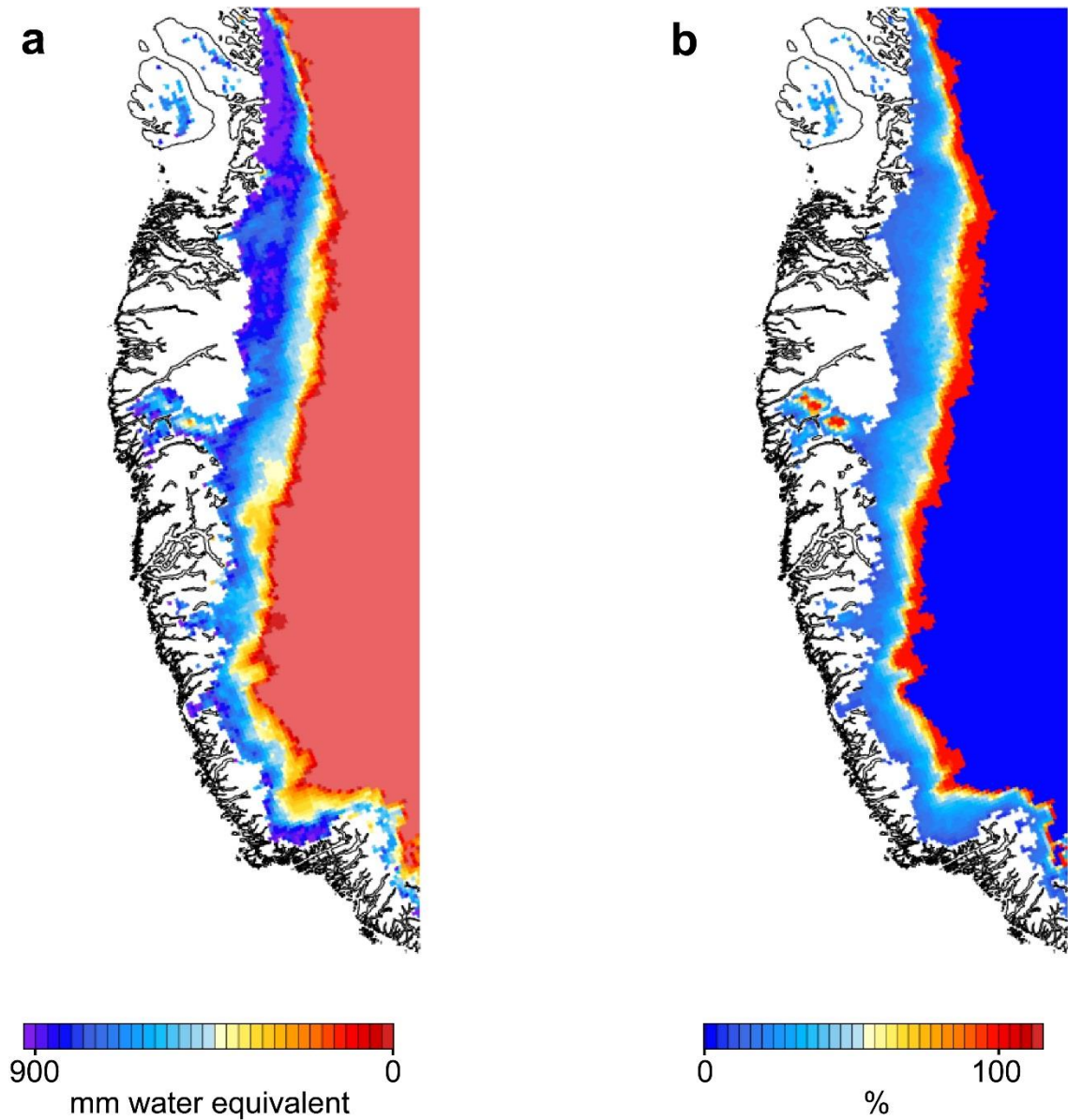


Figure 2. Results from the regional climate model over the ice-sheet covered part of Southwest Greenland. Panel a) The difference in runoff between 1980-1991 and 2003-2014 given in mm water equivalent (ie. the amount of water corresponding the ice melted away). Panel b) The same difference given in percent increase from the first period to the next.

Summing up the results from the regional climate model on a monthly basis within the model domain marked in Fig. 1 allows a quantification and evaluation of the total difference and its seasonal distribution (see Fig. 3). Fig. 3 illustrates that the relative difference is larger in the early and late parts of the melt season, as the latter is expanding, but also that the difference in terms of volume is larger from June to August. The total increase in the ice sheet meltwater runoff in Southwest Greenland is estimated to be 54% between the two 12-year periods 1980-1991 and 2003-2014.

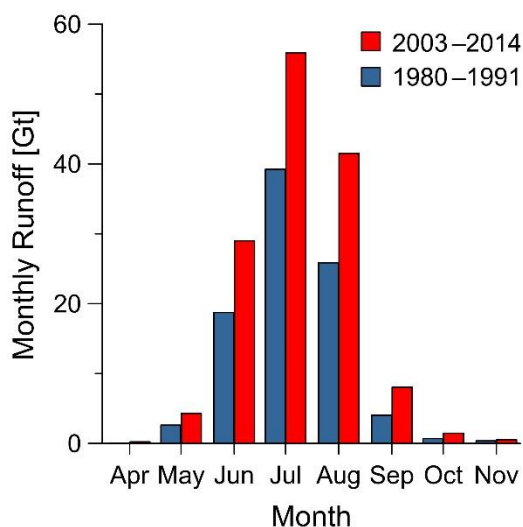


Figure 3. The estimated monthly mean runoff from the regional climate model for the ice-sheet covered part of the model domain (delimited in red in Fig. 1). The blue colour represents the period 1980-1991 and the red colour represents the period 2003-2014.

Model results from the ice-free terrain, illustrated in Fig. 4, are more relevant for the smaller catchments, often situated in the vicinity of populated areas. Fig. 4a shows a minor increase in the runoff from the ice-free terrain, typically varying between +1 and -1 mm water equivalent. The change in percent, shown in Fig. 4b, exhibits the same geographical distribution as seen in Fig. 4a. Evidently, the difference in runoff between the two 12-year periods is significantly smaller for the ice-free area than for the ice-sheet covered area, and varies over the region. The area in the vicinity the ice margin north of Nuup Kangerlua/Godthåbsfjorden has become more dry, while the area closer to the coast has become more wet. The area south of Nuup Kangerlua/Godthåbsfjorden has primarily become more dry, with a few exceptions.

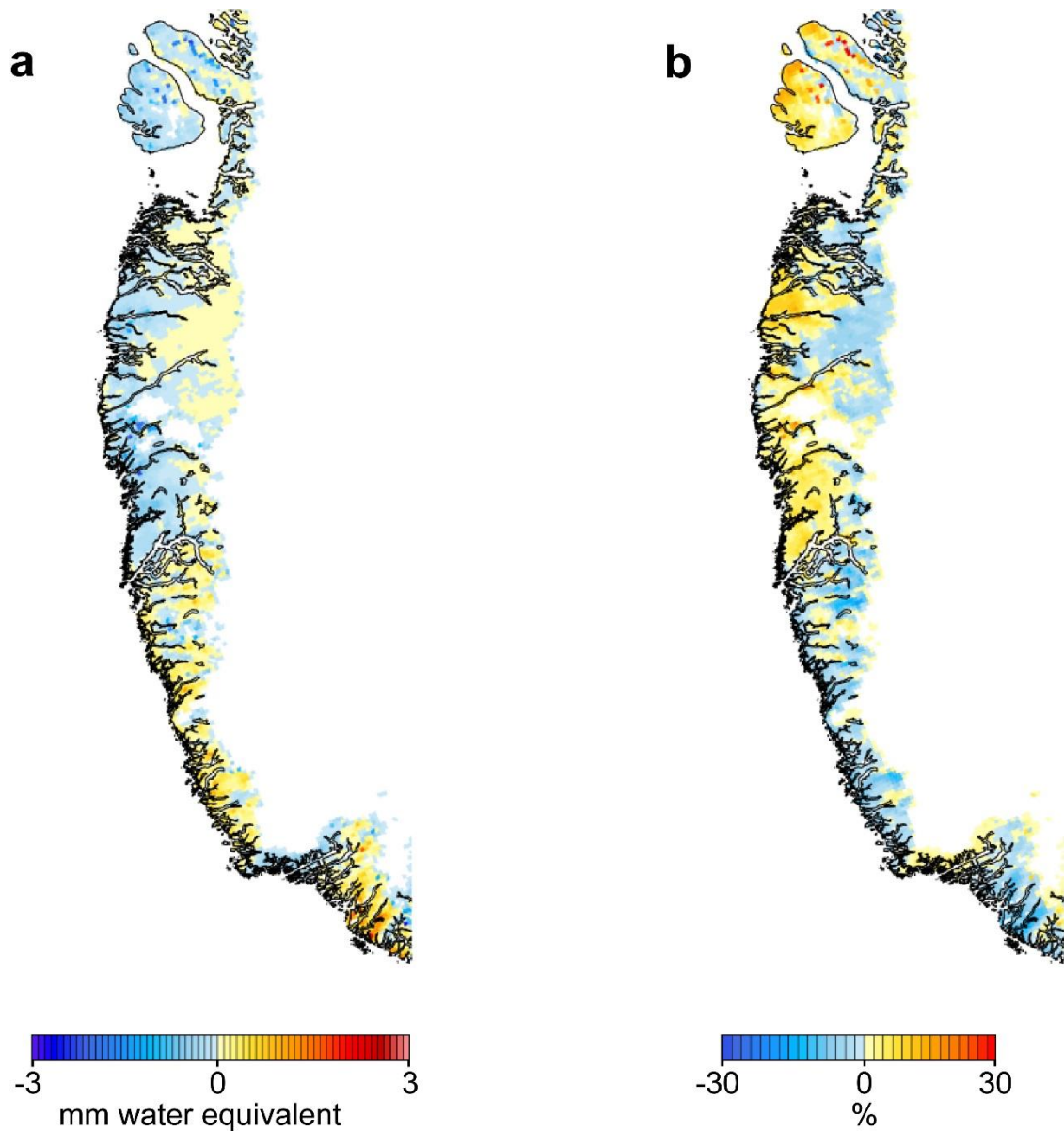


Figure 4. Results from the regional climate model over the ice-free part of Southwest Greenland. Panel a) The difference in land runoff between 1980-1991 and 2003-2014 given in mm water. Panel b) The same difference given in percent increase from the first period to the next.

Summing up instead the results from the regional climate model on a monthly basis for the ice-free part of the within the model domain marked in Fig. 1, it is evident that values are more than an order of magnitude smaller than for the ice-covered part (see Fig. 5). Meanwhile, we know from examining Fig. 4 that these values represent the sum of both negative and positive numbers and might thus cover potentially larger differences, which may be either positive or negative on local basis. However, the total shows an estimated increase in the runoff from the ice-free terrain of 33% between the two 12-year periods 1980-1991 and 2003-2014.

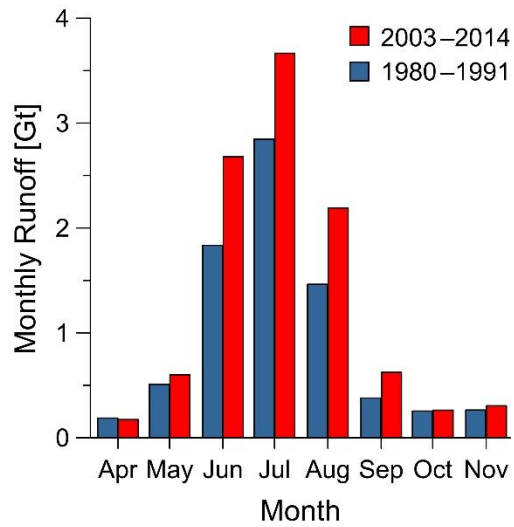


Figure 5. The estimated monthly mean runoff from the regional climate model for the ice-free part of the model domain (delimited in red in Fig. 1). The blue colour represents the period 1980-1991 and the red colour represents the period 2003-2014. While the numbers are more than an order of magnitude lower than for the ice-covered part of the model domain shown in Fig. 3, they specifically convey the total integrated difference over the entire ice-free part of the model domain, hiding possible local variations that may be either positive or negative (see Fig. 4).

Four previously assessed hydropower potentials

The focus of this report will be a new assessment of four previously assessed industrial-size hydropower potentials 07.d, 07.e, 07.f og 06.g (shown in Fig. 6), as we believe this to be the most efficient starting point for a new assessment of the hydropower potential of Greenland.

Three out of these four hydropower potentials are based on the assumption that several natural catchments will be connected in the development phase. In this assessment, we examine datasets retrieved from these natural catchments which are initially analysed separately and then subsequently combined in a final analysis of the evolution of the potentials.

Initially, we present the methods employed by Asiaq to calculate the discharge and by GEUS to delineate the catchments on the ice sheet and the ice-free terrain, respectively. Subsequently, we present for each catchment the data coverage, the establishment of a uniform time series covering 1980-2014 and finally the estimated water resource. The period 1980-2014 was chosen because it provides an adequate data coverage for intercomparison of the potentials. For establishing a complete time series, measured data provided the starting point, supplemented with bias-adjusted measured data from nearby catchments, or from the regional climate model HIRHAM5.

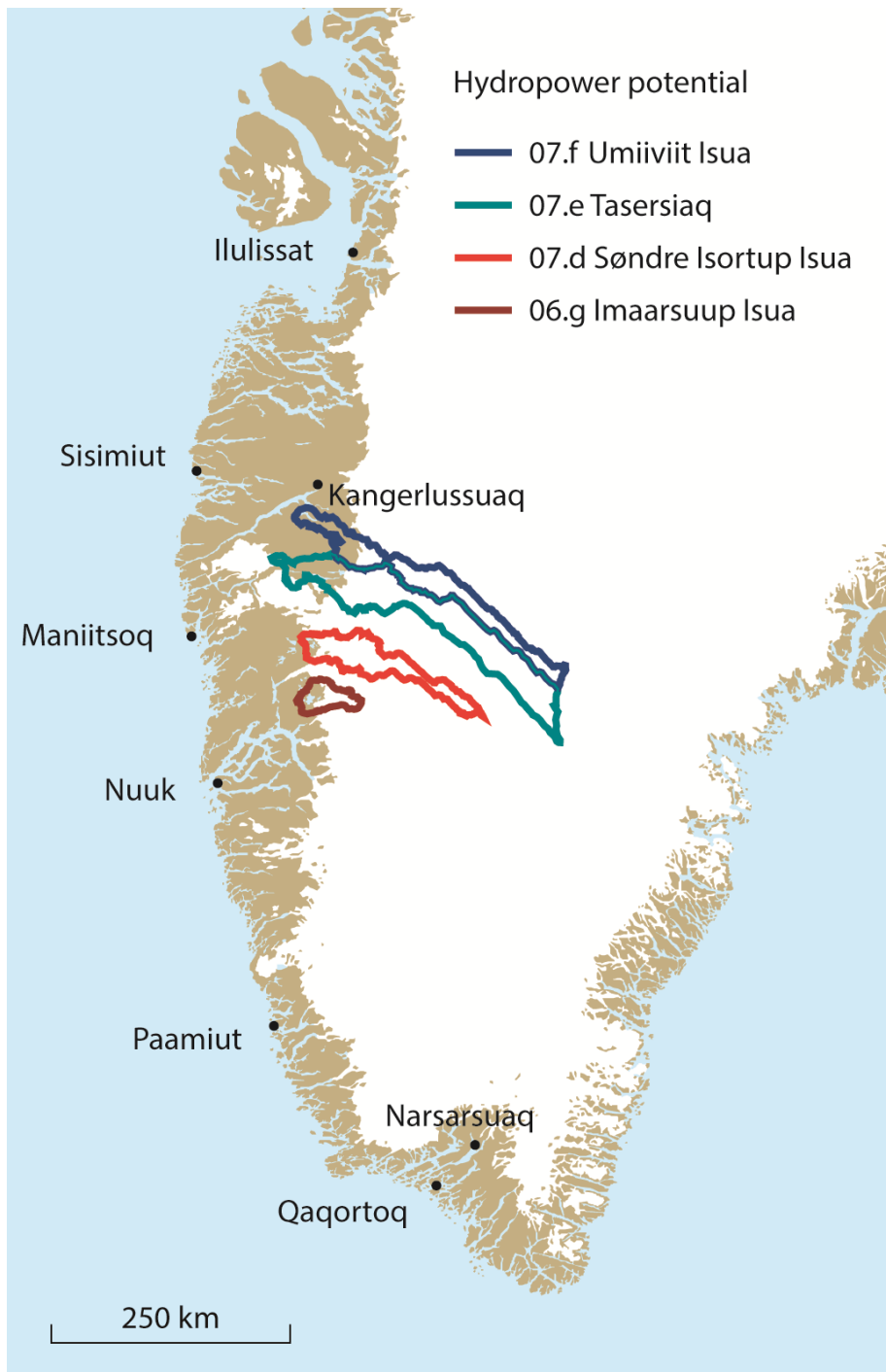


Figure 6. Four known hydropower potentials with capacity for industrial use.

Method

Measuring the water resource

The water resource at a catchment is evaluated as the mean annual discharge for that catchment, and is thus calculated from the discharge time series. The discharge time series is not measured directly but calculated indirectly from continuously measured water level and a stage-discharge relation, termed the Q/h-relation, specific to the location. The stage or water level is the absolute elevation of the water surface which varies according to the inflow of water. For lakes in Greenland, the water level is generally high during the summer and low during the winter. The difference between the water level in the summer and in the winter typically amounts to 1 to 3 metres, but for some lakes, the difference can be as large as 10 metres.

Water level registration

Water depth is monitored at an automatic measuring station by pressure transducers placed on the lake or river bottom. A picture of the hydrometric station monitoring catchment 07.d.I is shown in Fig. 1 as example. The water depth is measured daily or sub-daily. The water level of the lake or river is measured relative to a reference point (gauge datum) by levelling every time the station is visited. Based on the result of the leveling and the water depth measured simultaneously by the pressure transducer the position (height) of the sensor can be found. A time series of water level can thus be found from the sensor position and the measured water depth.



Figure 7. Hydrometric station monitoring catchment 07.d.I. Stations measures the water depth as well as selected climatic parameters (air temperature, wind speed and precipitation). The station is powered by solar panels and batteries. Data are stored in a data logger on site and transferred on a daily basis to Asiaqs office via an iridium satellite modem. Photo: Asiaq.

Stage-discharge relation

A stage-discharge relation is an empirical relation describing the discharge as a function of the height of the water surface (the water level). In general it is recommended to base the stage-discharge relation on at least 12 to 15 manual discharge measurements evenly distributed over the interval of water levels occurring at the site (ISO 1100-2). As a stage-discharge relation is an empirical relation extrapolation beyond the interval of manually measured discharges has a higher degree of uncertainty and should always be evaluated and used with great care. Especially extrapolation beyond the maximum manually measured discharge (upward extrapolation) can be problematic, whereas extrapolation to low values (downward extrapolation) is less problematic due to the lower constrain of zero discharge.

Manual discharge measurements

Discharge is measured manually by the velocity-area method (ISO 748). At a cross section of the river the water velocity is measured in a number of points in a number of verticals distributed over the cross section, see **Fejl! Henvisningskilde ikke fundet.8** for an example. Generally measurements are carried out in 15-20 verticals with measurements of water velocity in 1-4 points in each vertical depending on the water depth. The discharge is calculated by integration of the velocities over the cross sectional area.



Figure 8. Measurement of discharge at the outlet river from catchment 07.d.I. A wire is set up across the river at the measuring cross section and water velocity is measured by an acoustic Doppler current meter (ADCP) mounted on a small yellow catamaran boat, which can be seen near the opposite shore. Photo: Asiaq.

Time series of the water resource

Based on the time series of water level and the stage-discharge relation, a time series of discharge is calculated. Minor data gaps in the time series have been filled by linear interpolation. Data gaps outside of the melt-season have been filled by a mean basis runoff curve for the catchment. Outside of the melt season the discharge is generally very low and decreasing during the winter as the water storages (e.g. lakes) within the catchment are depleted. The discharge time series thus have a similar form each year although it can be somewhat shifted in time depending on the intensity of the melt season of that year.

The discharge time series is integrated to give annual discharge values. As the annual discharge can vary considerably from year to year depending on the climate it is recommended to base an evaluation of the water resource for a potential hydropower plant on a discharge time series covering 25 years (Nukissiorfiit, 2005). In this report we establish discharge time series for the 35-year period 1980-2014.

Filling of data gaps in measured time series

Regional climate models are not yet precise enough to be used to evaluate the water resource on catchment level directly (e.g. Teutschbein and Seibert (2012), Ehret et al. (2012)).

It is therefore necessary to adjust the model output, based on measured discharge for the catchment.

Annual model runoff values are compared with annual measured discharge values. For catchments where an adequate number of years of data is available, a linear regression is used as an adjustment function to adjust the annual model runoff values. For these catchments, it is found that HIRHAM5 typically captures the year-to-year variation well (correlation coefficients of 0.80-0.95), but overestimates the magnitude of the year-to-year variations (slope of 0.2-0.7, i.e. less than 1). Furthermore the linear regressions have non-zero offsets.

For some catchments the measured discharge time series is too short to base a linear regression on. In these cases, the ratio of measured annual values to modelled annual runoff are calculated for each year and the mean ratio is used to adjust the annual model runoff values.

Statistical evaluation

The Spearman's Rho test is a rank-based, non-parametric statistical test for detecting monotonic trends in time series. The Spearman's Rho test has similar power in detecting a trend as the Mann-Kendall test, which has often been used to test hydro-meteorological time series (Yue et al., 2002).

While non-parametric tests do not require the data to be normal distributed, they do require data to be serial independent (no autocorrelation). The disadvantage of the Spearman's Rho test is that it does not determine the size of the trend. To this end we have used the Theil-Sen slope estimator, which is a method that is robust and insensitive to outliers.

Delineation of catchments

The catchments are defined by the drainage area above the outlet, calculated using a standard GIS tools implemented in GRASS GIS (Neteler et al., 2012). The prior information used to calculate the catchments consists of a coordinate list of the outlets (Table 1), an elevation model of the Greenland ice sheet with a resolution of 30 m (GIMP DEM; Howat et al., 2014) and an elevation model of the area without ice, with a resolution of 5 m (ArcticDEM; Morin et al., 2016).

The first step when defining catchments, was to calculate the flow direction of an area enclosing all catchments, both the ice-covered area and the areas without ice, using the GIMP elevation model. The algorithm used to calculate the flow direction provides placement of streams as a raster file (a grid) and the flow direction of all grid cells in the GIMP elevation model.

The raster file containing the streams was converted into a vector format and exported as a KML-layer to be used in Google Earth. The calculated placement of the streams was compared to visible streams using Google Earth as the background. In areas where the comparison shows disagreement between the calculated and visible streams, the GIMP elevation model is manually edited by adding blockades, forcing the calculation to provide more realistic streams. Subsequently, the original outlet positions (Table 1) were shifted to be located in a grid cell with a calculated stream. The shift in outlet position was made to be congruent with the nearest significant stream. The shift was in general between 0-5 grid cells (0-200 m). The outlines of the catchments were then derived using the shifted outlet positions and calculations of flow direction. The process was repeated iteratively, until the calculated outlet positions were reasonably correct and the catchments were comparable to existing manually drawn maps.

Catchment ID	Longitude (°W)	Latitude (°N)
06.g.I	50.21426	64.93224
06.g.II	50.15527	65.15175
06.g.III	50.14664	65.15954
06.g.IV	49.92027	64.93000
07.d.I	50.33261	65.53874
07.d.II	50.28814	65.47091
07.e	51.31338	66.30535
07.f.I	51.11731	66.67358
07.f.II	49.78297	66.62143

Table 1. Geographical coordinates of the outlet positions of each catchment.

The next step involved improving the calculation of the catchment areas without ice, as the 30 m resolution provided by the GIMP elevation model is not sufficient to define the catchment outlines in landscapes with highly varying topography. The process outlined in the section above was repeated for the areas without ice, this time using the ArcticDEM elevation model, which has a resolution of 5 m. Again, the outlet positions were shifted to fit the calculated streams before deriving the upstream catchment.

Each catchment was then divided into an ice-covered part and land part (ice free) using an ice/land mask (Citterio & Ahlstrøm, 2013). The catchment based on the ArcticDEM was cut to fit the land part and the catchment based on the GIMP was cut to fit the ice part. The land part of the catchment (5 m resolution) was then resampled to 30 m resolution. The high resolution of 5 m gives a better calculation of the catchment outlines in the highly varying terrain, but is unnecessary after the calculation is done and has a very limited effect on the final result.

The catchment outlines were calculated using an 8-direction (D8) single flow direction model (SFD), which implies that all the water in one grid cell is assigned a single flow direction towards the steepest downslope neighboring grid cell. The assigned flow direction can only be towards one of the 8 neighboring grid cells. A comparison of the results from the SFD to a calculation using a multiple flow direction model (MFD) showed that the difference between the two was insignificant, remaining within a few grid cells at the edge of each catchment.

The results of the process explained above, were two masks for each catchment: a land mask and an ice mask. The next step was to use the masks to deduce the discharge from the regional climate model.

Error analysis of the catchment delineation

A catchment calculated with the method defined above is not necessarily the exact catchment for a given outlet. For the ice-covered part, the catchment will change when the ice surface changes. Additionally, the delineation of a catchment on the Greenland ice sheet will depend on the internal hydrological system of the ice, which in turn depends on the ice thickness and a number of other parameters such as the amount of added meltwater per time and the time-dependent evolution of the hydrological system at the base of the ice throughout the melt season.

Despite these shortcomings, we consider a delineation of the ice-covered part of the catchment based on the 30 m resolution GIMP elevation model to be a good approximation. This assumption is based on the currently available science (e.g. Ahlstrøm & Petersen and others, 2017) and visual comparison to surface meltwater streams visible in the Google Earth image layer. The visible meltwater rivers followed the above delineated catchments fairly well.

An alternative would be to utilize the best existing ice thickness model (Morlighem et al., 2017) in the analysis. However, this does not have an adequate resolution and underlying

data coverage to be sufficient on catchment scale (Morlighem, personal communication; Ahlstrøm & Petersen and others, 2017).

The land sector delineation within the catchments had large and significant errors in the first derivation based on the 30 m resolution GIMP elevation model, leading to the implementation of the ArcticDEM with its higher resolution of 5 m. Using the ArcticDEM generally improved the catchment delineation, but introduced other problems. Specifically, certain parts of the ArcticDEM contains no grid cell values ("NULL" values) which in our derivation were set to 0 m elevation. When these occur outside the catchment, they have no influence on the result; when occurring inside the catchment boundaries, they have no influence either, as the flow direction algorithm treats these gaps as lakes which in turn have no influence on the total water balance of the catchment (as described in the following section). However, when a data gap is connected to the actual catchment boundary, the algorithm will derive the flow around this. A comparison between ArcticDEM and the delineated catchment boundaries showed that this occurred in one instance, resulting in an error of approx. 100 grid cells, corresponding to 2.5 km²; an insignificant part of the catchment in question.

Model-based discharge

The discharge through the outlet of each catchment was calculated for the period 1980-2014 based on the results from the regional climate model HIRHAM5 (Langen et al., 2017), which provide the following variables on a daily time scale:

- Surface discharge (ice, ice + land)
- Rain
- Snowfall
- Snowmelt
- Evaporation

The model output was recalculated from its original 0.5° x 0.5° resolution to grid with a 5.5 km resolution in the same map projection as the GIMP and ArcticDEM elevation models. We mainly used the modelled surface discharge, but also calculated the precipitation over the ice-covered part of each catchment as:

Precipitation = evaporation + rain + snowfall

The projected 5.5 km grids of the ice-covered part with the HIRHAM5 output containing respectively surface discharge and precipitation were further regridded into the 30 m resolution GIMP elevation model. The coarser resolution of the HIRHAM5 model implies that its ice mask will not fit the 30 m resolution ice mask used in this analysis. To fill out the missing values of modelled discharge and precipitation occurring when applying the high resolution ice mask, a 3 x 3 grid cell box filter was used, where the cells without a value were given the mean of the valid neighboring cells (up to a maximum of 8 cells).

This method will provide a conservative estimate of the discharge, as the missing cells are situated at the part of the ice margin at the lowest elevation, where melting is expected to be more pronounced compared to the cells at higher elevation from which the boundary values are extrapolated.

Precipitation was only calculated for the ice-covered part of the catchments, as the HIRHAM5 precipitation output from the (generally small) areas without ice yielded rather noisy datasets of minimal importance for the compiled discharge. This again is a conservative choice, resulting in a slightly smaller calculated discharge.

An ice fraction value between 0 and 1 was assigned to each 5.5 km cell by evaluating the area with ice cover using the high resolution ice mask (30 m). The discharge of each 30 m cell was subsequently scaled to fit the area-based ice fraction. This provided another conservative estimate, as a 50/50 split of the area between ice/land will be scaled with 0.5 even though the largest part of the discharge in such conditions are likely to originate from the ice-covered part. Yet, the number of cells containing both ice and land is rather limited compared to the total number of cells in a catchment, making the influence on the calculated discharge relatively small.

Using the above-mentioned choices, the model-based daily total discharge was calculated for each catchment, as a combination of surface discharge and precipitation. In the measured time series, years without measurements occur. These data gaps were filled by the model-derived time series, as described in the next section. To this end, a correlation between the measured and model-derived time series was established in order to calibrate the latter with observations. Therefore, it is not crucial if the absolute values of the modelled discharge are correct, as long as the model is able to catch the variability of the time series.

Hydropower potential 06.g

The hydro power potential 06.g Imaarsuup Isua is based on four natural catchments marked as (I), (II), (III) and (IV) (see Fig. 9).

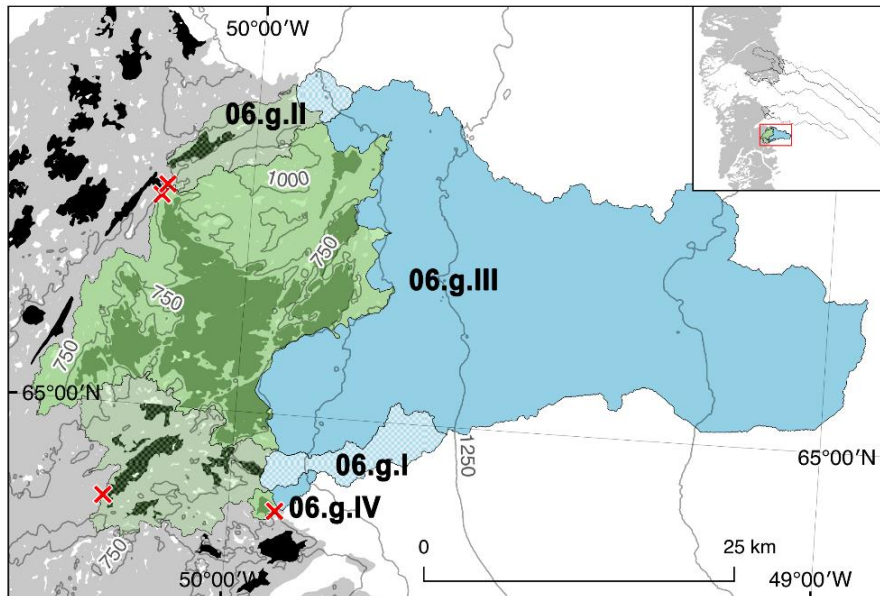


Figure 9. Map showing the four natural catchments marked with roman numerals I-IV, which combined represents the hydropower potential 06.g. All catchments are divided into a blue ice-covered area, a green area without ice and a red cross to mark the outlet.

Monitoring of the water resource

Investigations of hydropower potential 06.g were initiated in 1974 by Kryolitselskabet Øresund, as a possible power supply to a potential mine at the nearby iron ore at Isukasia (Kryolitselskabet Øresund 1984). Monitoring of the water resource was taken over by the Greenland Technical Organization (GTO) in 1985 and terminated in 1989. In 2008, monitoring of the water resource was started up again on initiative of the aluminium company Alcoa, due to a renewed interest in the hydropower potential as power supply for industry with high energy consumption. The monitoring was taken over by Asiaq – Greenland Survey in 2013 and is still ongoing as of 2018. The monitoring has focused on catchment (I) which contributes with around 82% of the total water resource for the hydropower potential (see Water resource section below).

Hydrometric stations have been established at each of the four catchments, but these have been operational for different periods of time. Stage-discharge relations have been established for each catchment based on manual discharge measurements (see Table 2). For

catchments 06.g.I and 06.g.II, the stage-discharge relations are based on a reasonable number of discharge measurements that covers the range discharge reasonably (extrapolation of the stage-discharge relation amount to less than 15% of the total discharge volume). For catchments 06.g.III and 06.g.IV, the few discharge measurements form a weak basis for the stage-discharge relations and measurements at low discharge are specifically lacking for catchment 06.g.III. However, as catchments 06.g.III and 06.g.IV only contributes with around 10% of the water resource, the uncertainty of their stage-discharge relations does not influence the evaluation of the total water resource for the hydropower potential to any significant degree.

An overview of the data coverage of the discharge time series for each catchment is given in Fig. 10.

Catchment ID	Manual discharge measurements	Part of total discharge volume found by extrapolation of stage- discharge relation or gap filling, %		
		Upward extrapolation	Downward extrapolation	Gap filling
06.g.I	14	3%	10%	4%
06.g.II	13	9%	1%	1%
06.g.III	4	4%	31%	1%
06.g.IV	5	9%	2%	0%

Table 2. Basis for the stage-discharge relation for each catchment and part of total discharge volume found by extrapolation of the stage-discharge relation or gap filling.

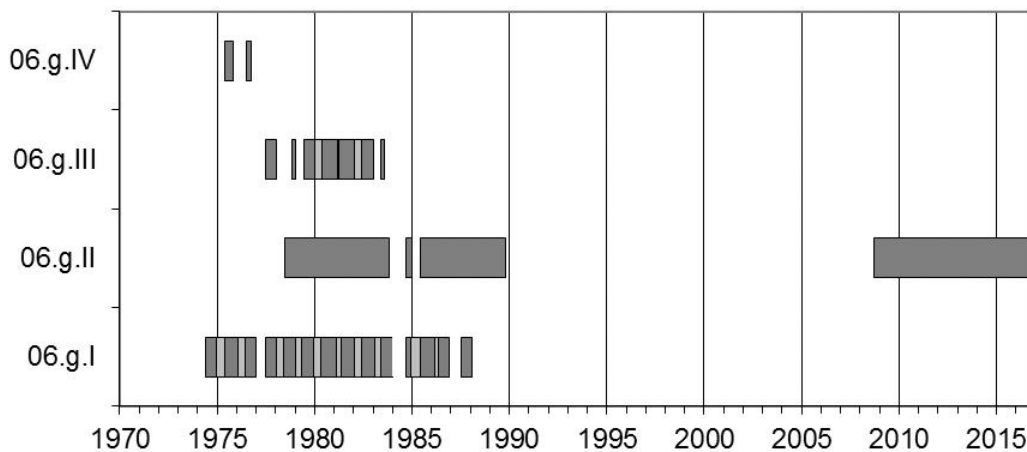


Figure 10. Data coverage of measured discharge time series for catchments in hydro-power potential 06.g. Periods with measured data are shown as dark grey bars, periods with larger, filled data gaps are shown with light grey bars (for description of gap filling method, see method section).

Establishing the 1980-2014 time series

The measured discharge time series does not cover the entire period from 1980 to 2014 in any of the sub-catchments shown in Fig. 10. Therefore, HIRHAM5 runoff data as well as discharge data from the nearby catchment 07.d.I is used to supplement the measured discharge time series.

For catchment 06.g.I, runoff from the ice-free parts of the catchment constitutes a significant part of the total runoff; 45% according to HIRHAM5. This is in contrast to the other catchments, where runoff from the ice covered part is dominant. For this reason, annual discharge values from 06.g.I does not correlate well with data from the neighboring catchment 06.g.II. The measured time series has five years overlapping with the HIRHAM5 time series and the correlation is fair ($R^2 = 0.40$). The 1980-2014 annual discharge time series is constructed with measured data supplemented with HIRHAM5 annual runoff values adjusted linearly by the regression formula.

For catchment 06.g.II, meltwater from the Greenland ice sheet (GrIS) dominates the discharge. In order to base the correlation with HIRHAM5 data on as large a dataset as possible, only modelled runoff from the ice-covered part of the catchment is considered, since the model output from land areas only covers 1980-2014, whereas the model output from the glacier-covered areas covers 1980-2016. The measured time series has 17 years overlapping with the HIRHAM5 ice runoff time series and the correlation is very good ($R^2 = 0.93$). The measured discharge from the period 2008-2012 is a restricted dataset and not to be made public. The 1980-2014 annual discharge time series is constructed with the non-restricted measured data, supplemented with HIRHAM5 annual runoff values adjusted linearly by the regression formula.

The main part of the measured discharge time series for catchment 06.g.III is measured previous to the period covered by HIRHAM5 model output. Therefore, the overlap between measurements and HIRHAM5 output is limited to two years, which is not sufficient to establish a reliable regression. The discharge from catchment 06.g.III correlates very well ($R^2 = 0.998$) with discharge from the neighboring catchment 06.g.II (based on data from five years). The 1980-2014 annual discharge time series is constructed with measured data, supplemented with data from 06.g.II 1980-2014 discharge time series adjusted linearly by the regression formula.

The measured discharge time series for catchment 06.g.IV covers the summers of 1975 and 1976 (see Fig. 10) and thus has no overlap with the HIRHAM5 output. The 06.g.IV data do overlap with measured discharge from catchment 06.g.I, but as the discharge from 06.g.IV is larger in 1975 than in 1976 (in contrast to the discharge from 06.g.I), it is unlikely that an adjusted 06.g.I time series will be a good estimator for the 06.g.IV discharge. This discrepancy is likely due to glacial meltwater being a much larger contribution to the discharge from 06.g.IV than from 06.g.I. We thus turn to catchment 07.d.I (see the section on Hydropower potential 07.d), which is situated around 40 km to the north of 06.g.IV. Here, the discharge in 1975 was larger than in 1976, as was the case at 06.g.IV. The mean ratio between annual discharge values has been used to adjust the 07.d.I annual time series to estimate the 1980-2014 annual discharge time series for catchment 06.g.IV.

The water resource

Based on the 1980-2014 discharge time series for the four catchments, the mean annual water resource at hydropower potential 06.g has been calculated to 1.08 km³ (see Table 3). Notably, the eight highest annual resource values occur within the period 2003-2014. The annual water resource shows a statistically significant, positive trend (significance level $p=0.01$) in a Spearman's Rho test. The trend for the discharge time series is estimated to be a 0.008 km³/year increase in discharge (Theil & Sen slope estimator).

Catchments	Annual water resource, km ³			Contribution to the water resource, %
	Average	Maximum	Minimum	
06.g.I	0.10	0.12	0.08	9
06.g.II	0.88	1.57	0.58	82
06.g.III	0.06	0.08	0.04	5
06.g.IV	0.04	0.08	0.03	4
06.g total	1.08	1.85	0.75	

Table 3. The water resource at hydropower potential 06.g.

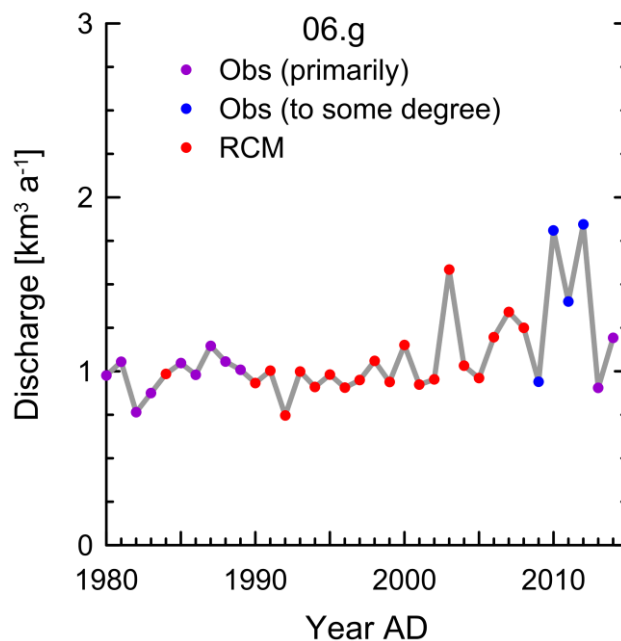


Figure 11. The annual discharge from the hydropower potentials 06.g with the following labelling of data sources; “Obs (primarily)”: mainly based on measured data, “Obs (to some degree)”: partially based on measured data, “RCM”: based on regression between results from climate models and measured data from other years.

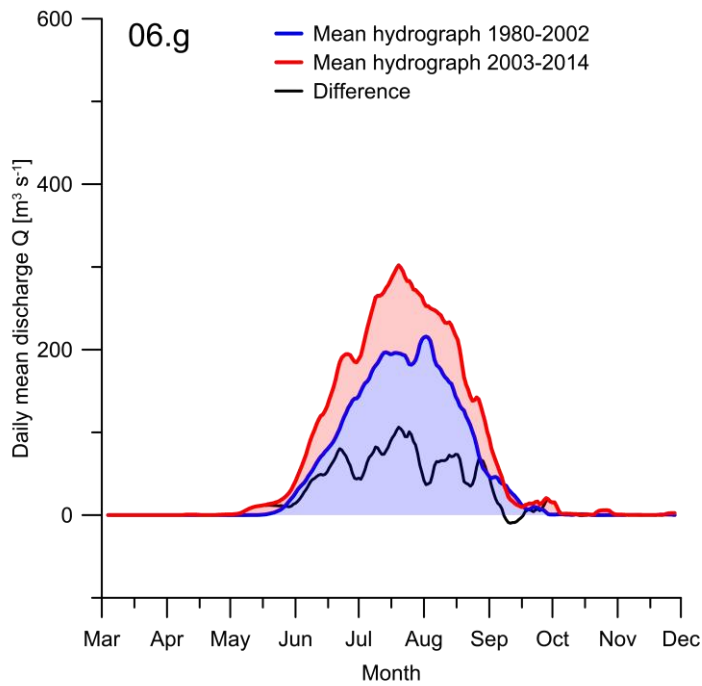


Figure 12. Mean hydrograph of the discharge from the hydropower potential 06.g during the periods 1980-2002 (blue) and 2003-2014 (red), respectively. The black curve illustrates the difference between the two periods.

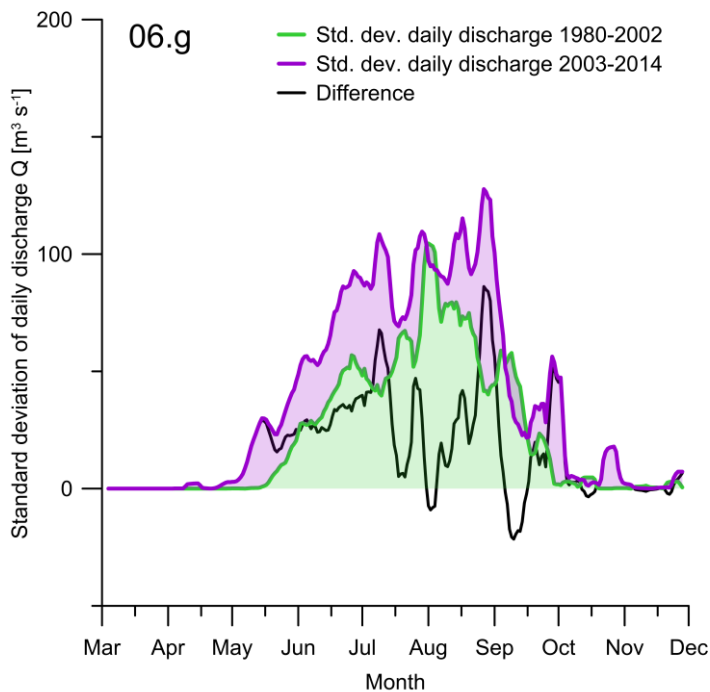


Figure 13. The standard deviation of the daily discharge (see Fig. 12) on any given day during the periods 1980-2002 (green) and 2003-2014 (purple). The difference between the periods is marked by the black curve.

Hydropower potential 07.d

The hydropower potential 07.d Søndre Isortup Isua is based on two natural catchments (I) and (II) (see Fig. 14).

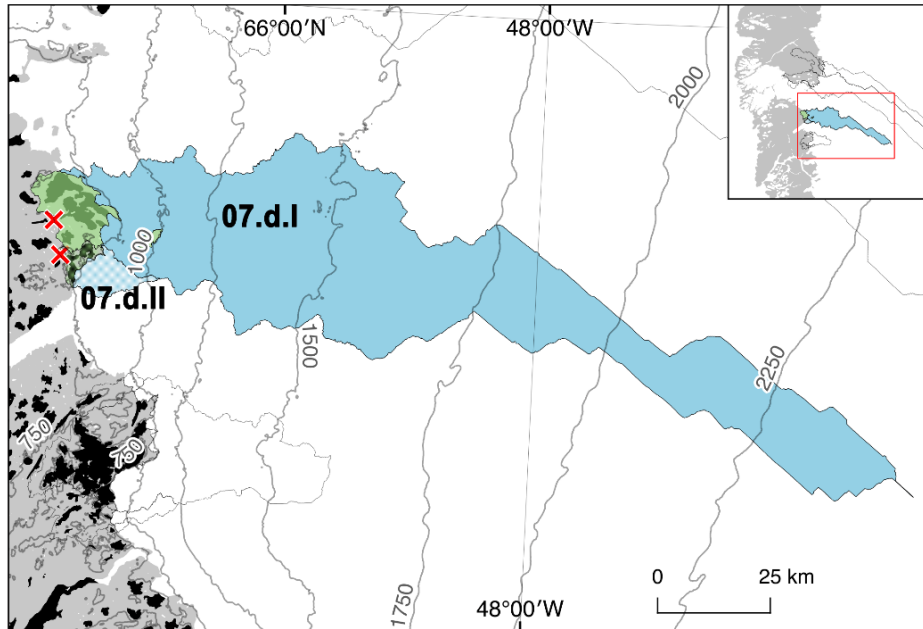


Figure 14. Map showing the two natural catchments marked with roman numerals I-II, which combined represents the hydropower potential 07.d. Both catchments are divided into a blue ice-covered area, a green area without ice and a red cross to mark the outlet.

Monitoring of the water resource

Investigations of hydropower potential 07.d were initiated in 1974 by Kryolitselskabet Øresund (Kryolitselskabet Øresund 1984) and terminated in 1983. In 2007, monitoring of the water resource was started up again on initiative of the aluminium company Alcoa, due to a renewed interest in the hydropower potential as power supply for industry with high energy consumption. The monitoring was taken over by Asiaq – Greenland Survey in 2009 and is still ongoing as of 2017.

In the early monitoring period from 1974-1983, only catchment 07.d.I. was included in the measuring program, whereas monitoring of both catchments, 07.d.I and 07.d.II, have been carried out since 2007. Stage-discharge relations have been established for each catchment based on manual discharge measurements (see Table 3). For catchment 07.d.I, the stage-discharge relation is based on a reasonable number of discharge measurements, although it would improve the accuracy of the resulting discharge time series if further manual discharge measurements at high discharge were carried out. This would reduce the derived amount of discharged water found by extrapolation of the stage-discharge relation to high

values. For catchment 07.d.II, the number of discharge measurement forming the base for the stage-discharge relation is in the lower end, but the coverage of the normally occurring discharges is sufficiently extensive (less than 3% of the total volume found by extrapolation).

An overview of the data coverage of the discharge time series for each catchment is given in Fig. 15.

Catchment ID	Manual discharge measurements	Part of total discharge volume found by extrapolation of stage discharge relation or gap filling, %		
		Upward extrapolation	Downward extrapolation	Gap filling
07.d.I	17	14%	2%	1%
07.d.II	9	0.3%	2%	0.3%

Table 4. Basis for the stage-discharge relation for each catchment and part of total discharge volume found by extrapolation of the stage-discharge relation or gap filling.

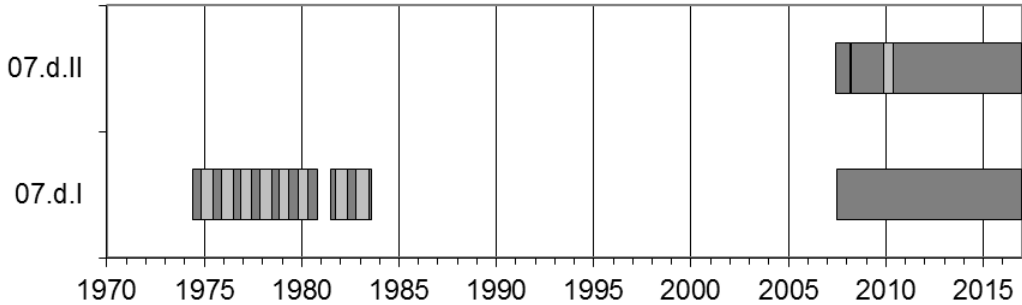


Figure 15. Data coverage of measured discharge time series for catchments in hydro-power potential 06.g. Periods with measured data are shown as dark grey bars, periods with larger, filled data gaps are shown with light grey bars (for description of gap filling method, see method section).

Establishing the 1980-2014 time series

The measured discharge time series does not cover the entire period from 1980 to 2014 in any of the sub-catchments shown in Fig. 15. Therefore, HIRHAM5 runoff data is used to supplement the measured discharge time series.

For catchment 07.d.I, meltwater from the Greenland ice sheet (GrIS) dominates the discharge. In order to base the correlation with HIRHAM5 data on as large a dataset as possible only modelled runoff from the ice-covered part of the catchment is considered since the model output from land areas only covers 1980-2014, whereas the model output from the glacier covered areas covers 1980-2016. The measured time series has 11 years overlapping with the HIRHAM5 ice runoff time series and the correlation is very good ($R^2 = 0.95$). The measured discharge in the period 2007-2008 2012 is a restricted dataset and not to be

made public. The 1980-2014 annual discharge time series is constructed with the non-restricted measured data, supplemented with HIRHAM5 annual runoff values adjusted linearly by the regression formula.

For catchment 07.d.II, the measured data series covers 10 years. The correlation between 07.d.II and 07.d.I is slightly better ($R^2 = 0.88$) than the correlation between 07.d.II and HIRHAM5 ($R^2 = 0.84$) and thus data from 07.d.I is used to fill data gaps. The measured discharge in the period 2007-2008 is a restricted dataset and not to be made public. The 1980-2014 annual discharge time series is constructed with the non-restricted measured data, supplemented with 07.d.I annual runoff values adjusted linearly by the regression formula.

The water resource

Based on the 1980-2014 discharge time series for the two catchments the mean annual water resource at hydropower potential 07.d has been calculated to 1.17 km³ (see Table 5). Notably, the eight highest annual resource values occur within the period 2003-2014. The annual water resource shows a statistically significant, positive trend (significance level $p=0.001$) in a Spearman's Rho test. The trend for the discharge time series is estimated to be a 0.009 km³/year increase in discharge (Theil & Sen slope estimator).

Catchments	Annual water resource, km ³			Contribution to the water resource, %
	Mean	Maximum	Minimum	
07.d.I	1.00	1.94	0.71	86
07.d.II	0.17	0.28	0.13	14
07.d total	1.17	2.22	0.84	

Table 5. The water resource at hydropower potential 07.d.

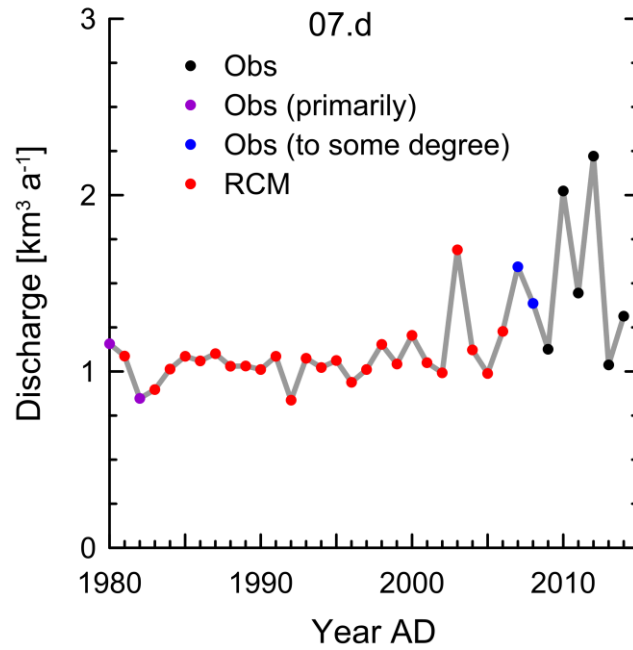


Figure 16. The annual discharge from the hydropower potential 07.d with the following labelling of data sources; “Obs”: measured data, “Obs (primarily)”: mainly based on measured data, “Obs (to some degree)”: partially based on measured data, “RCM”: based on regression between results from climate models and measured data from other years.

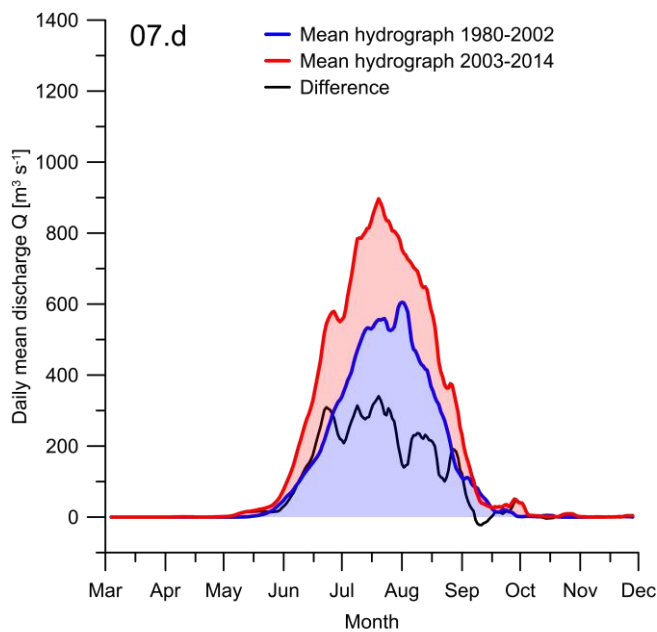


Figure 17. Mean hydrograph of the discharge from the hydropower potential 07.d during the periods 1980-2002 (blue) and 2003-2014 (red), respectively. The black curve illustrates the difference between the two periods.

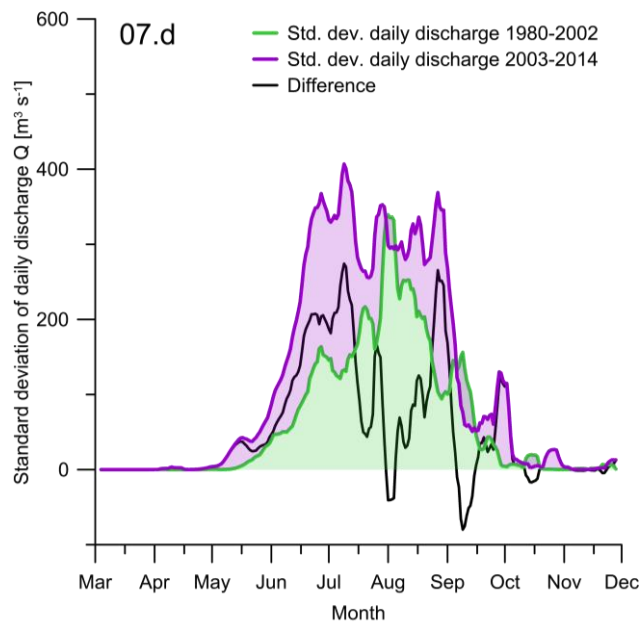


Figure 18. The standard deviation of the daily discharge (see Fig. 17) on any given day during the periods 1980-2002 (green) and 2003-2014 (purple). The difference between the periods is marked by the black curve.

Hydropower potential 07.e

The hydropower potential 07.e is based on exploitation of the catchment of lake Tasersiaq (see Fig. 19).

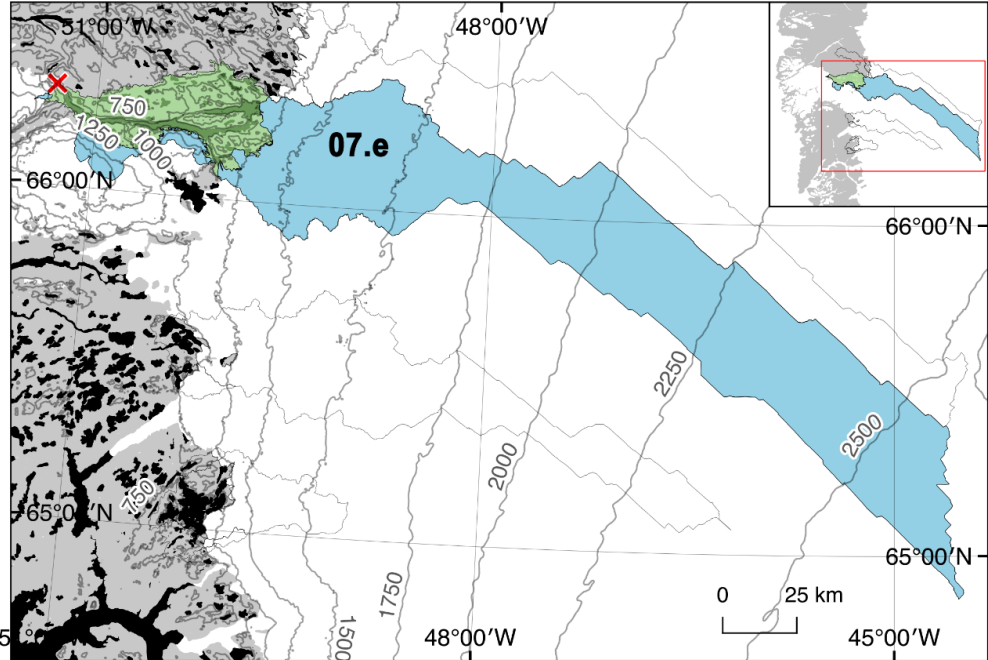


Figure 19. Map showing the hydropower potential 07.e. The catchment is divided into a blue ice-covered area, a green area without ice and a red cross to mark the outlet.

Monitoring of the water resource

Investigations of hydropower potential 07.e were initiated in 1975 by the Greenland Technical Organization (GTO) and is still ongoing as of 2018. Today the monitoring is run by Asiaq – Greenland Survey.

The stage-discharge relation for catchment 07.e is well-defined, as it is based on 37 manual discharge measurements, which covers the range of discharge from the catchment well (see Table 6). An overview of the data coverage of the discharge time series for each catchment is given in Fig. 20.

Catchment ID	Manual discharge measurements	Part of total discharge volume found by extrapolation of stage-discharge relation or gap filling, %		
		Upward extrapolation	Downward extrapolation	Gap filling
07.e	37	6%	1%	1%

Table 6. Basis for the stage-discharge relation for the catchment and part of total discharge volume found by extrapolation of the stage-discharge relation or gap filling.

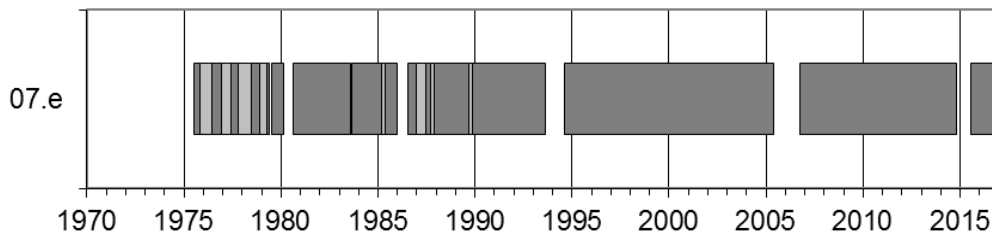


Figure 20. Data coverage of measured discharge time series for hydropower potential 07.e. Periods with measured data are shown as dark grey bars, periods with larger, filled data gaps are shown with light grey bars (for description of gap filling method, see method section).

Establishing the 1980-2014 time series

Although catchment 07.e has been monitored since 1975, some data gaps occur in the discharge time series and these has to be filled in order to generate the 1980-2014 time series. Therefore HIRHAM5 runoff data is used to supplement the measured discharge time series.

The discharge time series from catchment 07.e is dominated by the annual melt peak, but besides from this, the discharge time series exhibit occasional short-term peaks that occurs at all times of the year, but are most common in the autumn. The source is glacial lake outburst floods (GLOFs) from an upstream ice-dammed lake found at position N66°09', W050°54'. The time between GLOFs is normally a few years. This storage of meltwater from one year to another is not included in the HIRHAM5 model. Thus, the volume of water released at the GLOF events were removed from the measured discharge time series prior to the regression of measured and model annual annual values,. The measured time series has 29 years overlapping with the HIRHAM5 ice runoff time series with a strong correlation ($R^2 = 0.90$).

Missing annual values were estimated from HIRHAM5 annual runoff values adjusted linearly by the regression formula, with subsequent addition of the volume of water released during a given GLOF occurring in that year. By utilizing the relation between GLOF volume and the sum of positive degree days between events together with Landsat images, it has been possible to clarify that two GLOF events have taken place, which are not documented in the Tasersiaq discharge time series due to data gaps. The volume of water released during GLOF events decreases over time ($R^2 = 0.75$) due to thinning of the glacier damming the source lake of the GLOFs. The volume of water released during the two GLOF events that were not captured in the measured discharge time series, were estimated based on this relation.

The water resource

Based on the 1980-2014 discharge time series, the mean annual water resource at hydropower potential 07.e has been calculated to 2.78 km³ (see Table 6). Notably, the eight highest annual resource values occur within the period 2003-2014. The annual water resource

shows a statistically significant, positive trend (significance level $p < 0.0005$) in a Spearman's Rho test. The trend for the discharge time series is estimated to be a 0.056 km³/year increase in discharge (Theil & Sen slope estimator).

Catchment	Annual water resource, km ³		
	Average	Maximum	Minimum
07.e	2.78	6.81	0.61

Table 7. The water resource at hydropower potential 7.e.

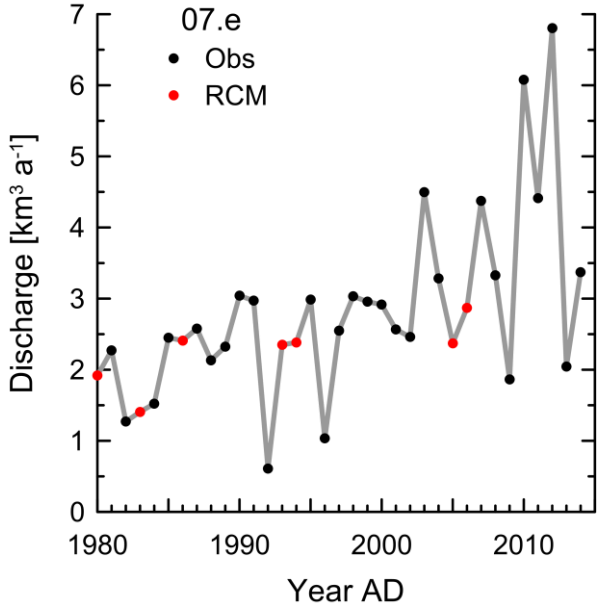


Figure 21. The annual discharge from the hydropower potential 07.d with the following labelling of data sources; “Obs”: measured data, “RCM”: based on regression between results from climate models and measured data from other years.

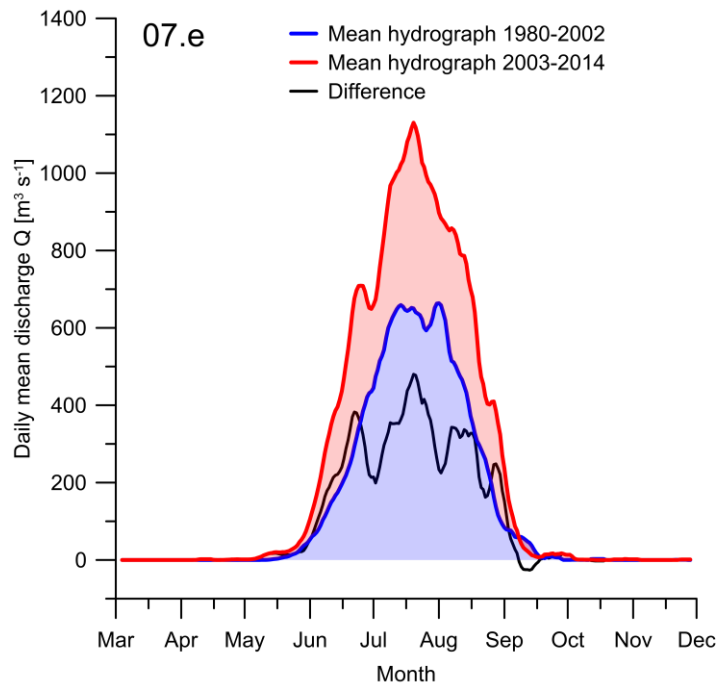


Figure 22. Mean hydrograph of the discharge from the hydro-power potential 07.e during the periods 1980-2002 (blue) and 2003-2014 (red), respectively. The black curve illustrates the difference between the two periods.

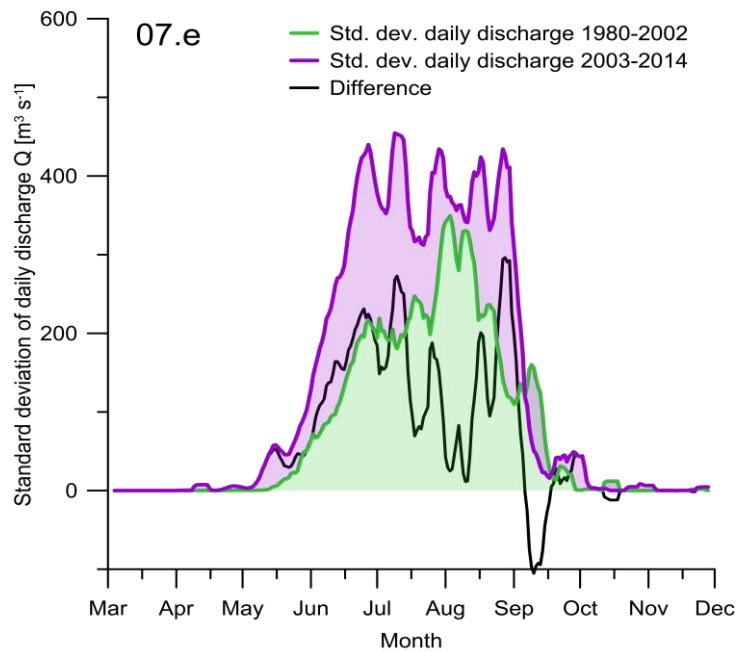


Figure 23. The standard deviation of the daily discharge (see Fig. 22) on any given day during the periods 1980-2002 (green) and 2003-2014 (purple). The difference between the periods is marked by the black curve.

Hydropower potential 07.f

The hydro power potential 07.f Umiiviit Isua is based on two natural catchments marked as (I) and (II) (see Fig. 24).

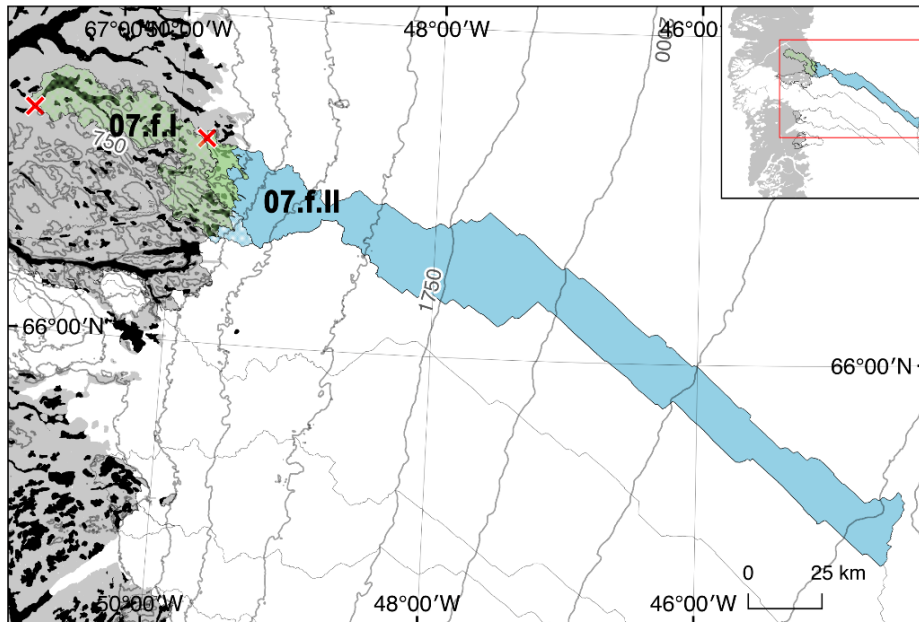


Figure 24. Map showing the two natural catchments marked with roman numerals I-II, which combined represents the hydropower potential 07.f. Both catchments are divided into a blue ice-covered area, a green area without ice and a red cross to mark the outlet.

Monitoring of the water resource

Investigations of hydropower potential 07.f were initiated in 1975 by the Greenland Technical Organization (GTO), when a hydrometric station was established at the river of catchment 07.f.II. The monitoring was closed down again in the autumn of 1976. Another hydrometric station was established at catchment 07.f.II in 1994 and kept in operation until 2002.

Stage-discharge relationships have been established for each catchment, based on manual discharge measurements (see Table 8). For both catchments, the stage-discharge relations are based on a very limited number of discharge measurements. Furthermore, catchment 06.f.I especially misses manual discharge measurements at low flow.

An overview of the data coverage of the discharge time series for each catchment is given in Fig. 25.

Catchment ID	Manual discharge measurements	Part of total discharge volume found by extrapolation of stage- discharge relation or gap filling, %		
		Upward extrapolation	Downward extrapolation	Gap filling
07.f.I	6	6%	32%	3%
07.f.II	3	6%	2%	

Table 8. Basis for the stage-discharge relation for each catchment and part of total discharge volume found by extrapolation of the stage-discharge relation or gap filling.

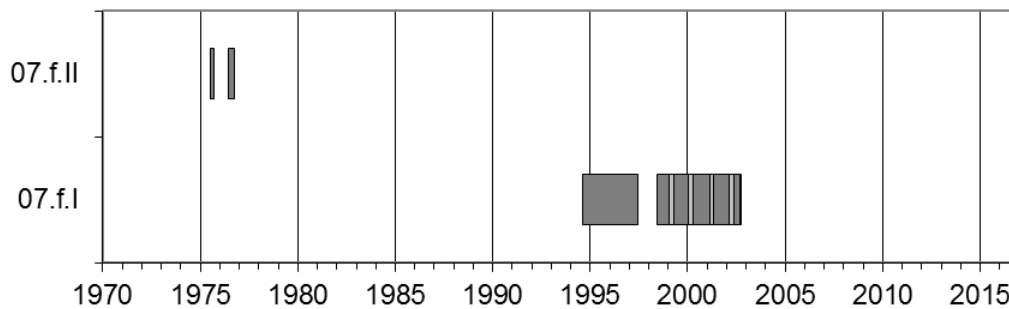


Figure 25. Data coverage of measured discharge time series for catchments in hydro-power potential 06.g. Periods with measured data are shown as dark grey bars, periods with larger, filled data gaps are shown with light grey bars (for description of gap filling method, see method section).

Establishing the 1980-2014 time series

The measured discharge time series does not cover the entire period from 1980 to 2014 in any of the sub-catchments shown in Fig. 25.

For catchment 07.f.I, runoff from the ice-free parts of the catchment constitutes a significant part of the total runoff; 52% according to HIRHAM5. This is in contrast to the neighbouring catchment 07.e, where runoff from the ice-covered part is dominant. Consequently, annual discharge values from 07.f.I does not correlate at all with data from 07.e. The measured time series has six years overlapping with the HIRHAM5 time series, but the correlation is poor ($R^2 = 0.04$). A somewhat better correlation ($R^2 = 0.42$) can be obtained by combining HIRHAM5 runoff for the ice-covered part of the catchment, with an estimate of the land runoff (based on precipitation data from Kangerlussuaq) multiplied by the ice-free catchment area. While this indicates that the HIRHAM5 land runoff may be quite uncertain, the measured discharge time series for catchment 07.f.I is not ideal either, as it is based on a weak stage-discharge relation (see the previous chapter). We therefore chose to base the 1980-2014 annual discharge time series on measured data, supplemented with HIRHAM5 annual runoff values adjusted by the mean ratio of measured to model annual discharge values.

The measured discharge time series for catchment 07.f.II covers the summers of 1975 and 1976 (Fig. 6) and thus has no overlap with the HIRHAM5 data. Fortunately, catchment 07.e (see the section on Hydropower Potential 07.e), which is situated around 40 km south of

07.f.II, has an overlapping time series. Furthermore, meltwater from the GrIS dominates the water resource for both catchments. The mean ratio between annual discharge values has been used to adjust the 07.e annual time series to estimate the 1980-2014 annual discharge time series for catchment 07.f.II.

The water resource

Based on the 1980-2014 discharge time series for the two catchments, the mean annual water resource at hydropower potential 07.f has been calculated to 1.35 km³ (see Table 9). Note that the water resource for 07.f is based on a very short measured time series and that the stage-discharge relations used to calculate the discharge time series are not well documented.

Notably, the eight highest annual resource values occur within the period 2003-2014. The annual water resource shows a statistically significant, positive trend (significance level $p < 0.0005$) in a Spearman’s Rho test. The trend for the discharge time series is estimated to be a 0.025 km³/year increase in discharge (Theil & Sen slope estimator).

Catchments	Annual water resource, km ³			Contribution to the water resource, %
	Average	Maximum	Minimum	
07.f.I	0.26	0.35	0.20	19
07.f.II	1.09	2.64	0.25	81
07.f total	1.35	2.99	0.49	

Table 9. *The water resource at hydropower potential 07.f.*

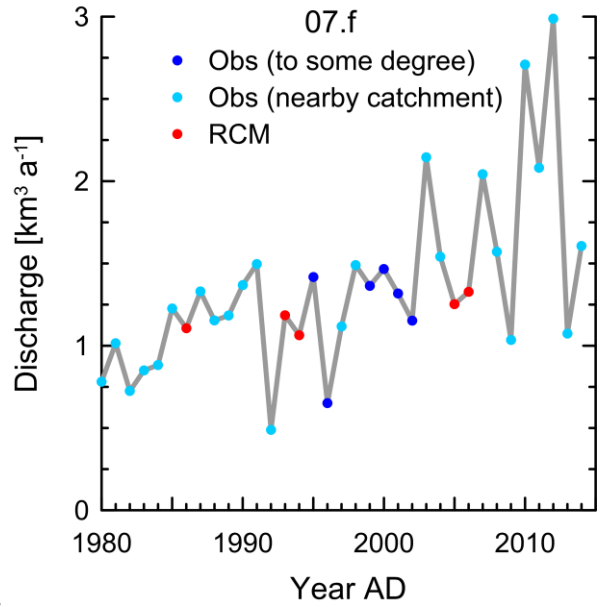


Figure 26. The annual discharge from the hydro-power potential 07.d with the following labelling of data sources; “Obs (to some degree)”: partially based on measured data, “Obs (nearby catchment)”: based on regression between measured data from catchments nearby and measured data from other years, “RCM”: based on regression between results from climate models and measured data from other years.

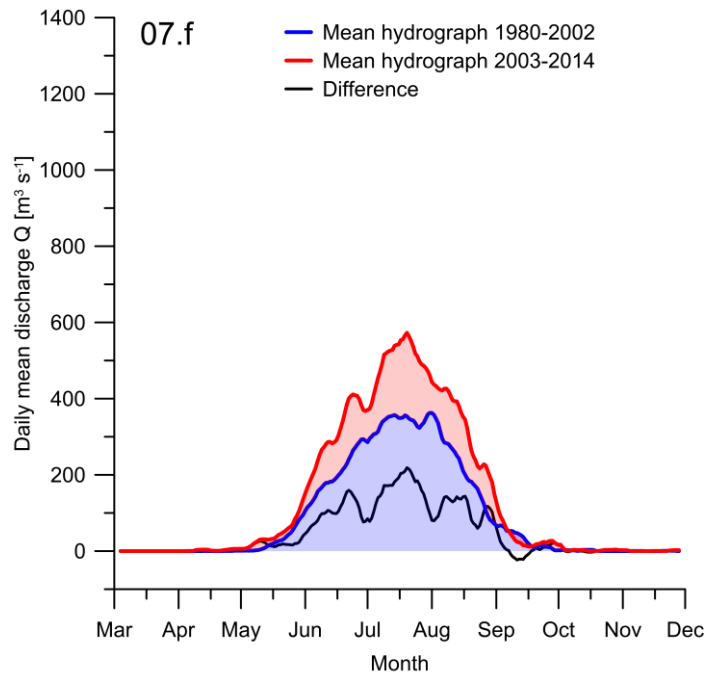


Figure 27. Mean hydrograph of the discharge from the hydro-power potential 07.f during the periods 1980-2002 (blue) and 2003-2014 (red), respectively. The black curve illustrates the difference between the two periods.

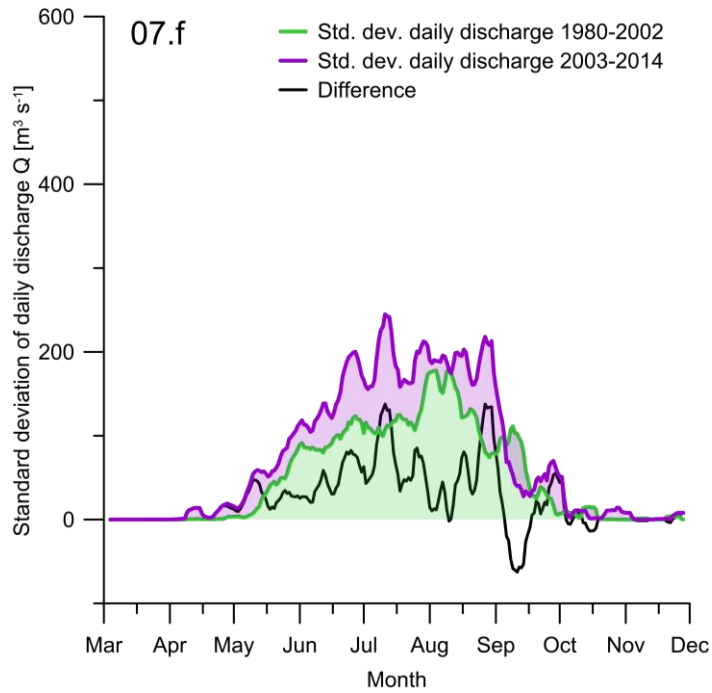


Figure 28. The standard deviation of the daily discharge (see Fig. 27) on any given day during the periods 1980-2002 (green) and 2003-2014 (purple). The difference between the periods is marked by the black curve.

Conclusion

Accessible water resources in Southwest Greenland have seen a remarkable change over the last decade, as documented in this report and in Ahlstrøm & Petersen and others (2017). Analyzing the reasons behind this change, Ahlstrøm & Petersen and others (2017) found that the origins of the air masses arriving over the catchment in the summertime seems to be shifting southwards, consequently carrying more heat and moisture. This leads to intensified summertime melting on the ice sheet surface, with a significant influence on the large hydropower potentials where the water resource primarily depends on the amount of meltwater runoff.

The changes in the general atmospheric circulation, leading to an intensified meridional transport of heat and moisture is believed to be due to global warming. On catchment scale, the result of this is a significantly larger mean annual discharge and a slightly longer melt season, but also a significantly higher variability in the discharge. All these parameters should be considered in future considerations of the exploitation of the water resource for hydropower. Although a connection to global climate change has been pointed out, it should be kept in mind that a part of these changes may be due to natural variability, e.g. in the ocean circulation. Thus, an investigation into the future development of the water resource must include model results based on the most likely climate scenarios, incorporating knowledge of both natural and anthropogenic climate change.

In this updated evaluation of the available water resource for the four large hydropower potentials of industrial interest in Southwest Greenland, 06.g, 07.d, 07.e and 07.f, we see the same overall development towards more discharge and higher variability over the last decade, as illustrated in Fig. 29. However, this change is more pronounced for the two most northerly hydropower potentials (07.e and 07.f) which are situated on the lee side of a topographical barrier, leading to less sensitivity to precipitation and more sensitivity to increased amounts of meltwater from the Greenland ice sheet (see Table 10 and 11). The current evaluation covers the development over the period 1980-2014, but data from the potential 07.e for 1975-1979 published in Ahlstrøm & Petersen and others (2017) does not change the conclusion. Table 10 and 11 describes the absolute and the relative rise in the water resource from two earlier periods, respectively, namely 1980-2002 (Table 10) and 1980-1991 (Table 11) and up to the period 2003-2014. The latter period was chosen because it has been identified as a possible new climatic state in Ahlstrøm & Petersen and others (2017). The period 1980-2002 just represents all the years prior to the shift in 2003 where regional climate model results are available, whereas the period 1980-1991 has been included to provide a comparison on catchment scale with the initial evaluation of the development of the water resources from all of Southwest Greenland.

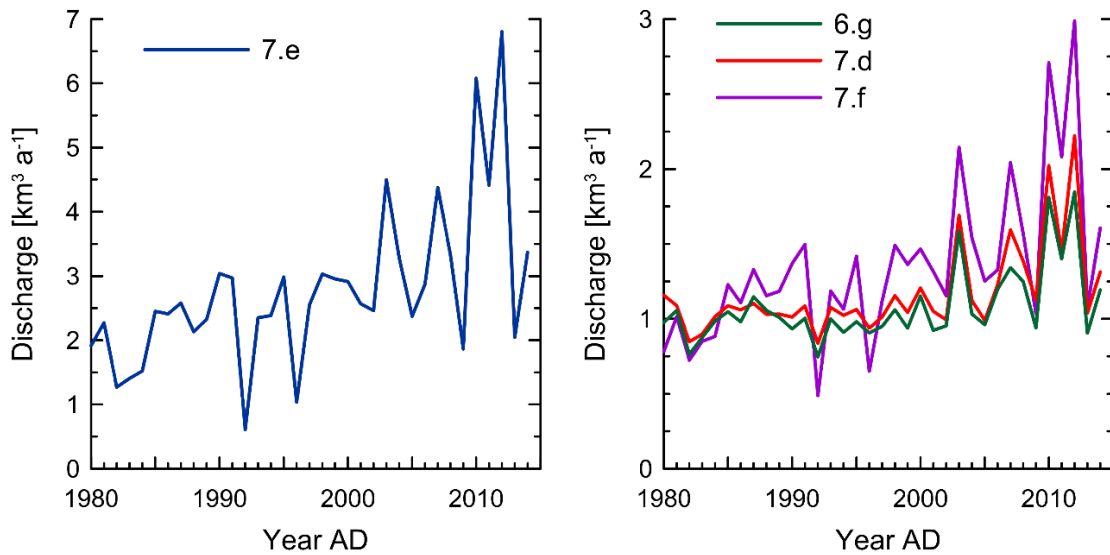


Figure 29. The annual discharge for the period 1980-2014 as estimated in this report. Note that the two graphs have different scales. The change in discharge after 2002 is quantified in Table 10.

Catchment	Discharge km ³ /yr 1980-2002	Discharge km ³ /yr 2003-2014	Increase in %
06.g	0.97	1.29	33
07.d	1.03	1.43	38
07.e	2.27	3.77	66
07.f	1.12	1.78	59

Table 10. Change in the discharge for the four hydropower potentials from the period 1980-2002 to the period 2003-2014.

Catchment	Discharge km ³ /yr 1980-1991	Discharge km ³ /yr 2003-2014	Increase in %
06.g	0.99	1.29	31
07.d	1.03	1.43	38
07.e	2.19	3.77	72
07.f	1.09	1.78	63

Table 11. Change in the discharge for the four hydropower potentials from the period 1980-1991 to the period 2003-2014.

A change in the water resource is not equivalent to a corresponding change in the possible energy production from the hydropower potential. The change in energy production is influenced by the relation between the annual discharge and the potential size of the storage, causing a non-linear relation through the resulting adjustment factor. Other technical assumptions include expected efficiency, fall height, pipes and type of turbines, and operating

time per year. Generally, an increase in the water resource would yield a lower degree of regulation and thus a lower adjustment factor, implying a less efficient utilization of the given water resource. It is thus possible, that the relative increase in the water resource documented in this report could result in a lower relative increase in the theoretically possible energy production.

References

- Ahlstrøm, A. P., D. Petersen, R. S. Fausto, P. L. Langen (2017) *En analyse af behovet for en ny kortlægning af Grønlands vandkraftresurser*, GEUS-Notat 10-NA-17-01, 10 pp.
- Ahlstrøm, A.P.* , D. Petersen*, P.L. Langen, M. Citterio, J.E. Box (2017) *Abrupt shift in the observed runoff from the southwestern Greenland ice sheet*, *Science Advances*, 3: e1701169.
- AMAP (2017) *Snow, Water, Ice and Permafrost. Summary for Policy-makers*, Arctic Monitoring and Assessment Programme (AMAP), Oslo, Norway. 20 pp.
- Citterio, M. and A.P. Ahlstrøm (2013) *Brief communication: The aerophotogrammetric map of Greenland ice masses*, *The Cryosphere*, 7, 445-449, 2013, doi:10.5194/tc-7-445-2013.
- Ehret, U., E. Zehe, V. Wulfmeyer, K. Warrach-Sagi and J. Liebert (2012) *Should we apply bias correction to global and regional climate model data?* *Hydrol. Earth Syst. Sci.*, 16, 3391–3404, 2012, doi:10.5194/hess-16-3391-2012.
- Howat, I.M., A. Negrete, B.E. Smith (2014) *The Greenland Ice Mapping Project (GIMP) land classification and surface elevation data sets*, *The Cryosphere* 8 (4), 1509-1518, doi: 10.5194/tc-8-1509-2014.
- International Hydropower Association (2017) *2017 Hydropower Status Report*, London, UK, 81 pp.
- ISO 748 *Measurements of liquid flow in open channels – velocity-area methods*, International standard. Third Edition. 1997-08-01.
- ISO 1100-2 *Measurement of liquid flow in open channels. Part 2: Determination of the stage-discharge relation*, International standard. Second Edition 1998-05-01.
- Kryolitselskabet Øresund (1984) *Isukasia Hydro-power. Field Investigations*, Artic Consultant Group. Vattenbyggnadsbyrå.
- Langen, P.L., R.S. Fausto, B. Vandecrux, R.H. Mottram, J.E. Box (2017) *Liquid Water Flow and Retention on the Greenland Ice Sheet in the Regional Climate Model HIRHAM5: Local and Large-scale Impacts*, *Frontiers in Earth Science* 4, doi: 10.3389/feart.2016.00110.
- Morin, P., C. Porter, M. Cloutier, I. Howat, M.-J. Noh, M. Willis, B. Bates, C. Williamson, K. Peterman (2016) *ArcticDEM; A Publically Available, High Resolution Elevation Model of the Arctic*, EGU General Assembly Conference Abstracts, Vol. 18, 8396.

* Shared first authorship.

Morlighem, M., C. N. Williams, E. Rignot, L. An, J. E. Arndt, J. L. Bamber, G. Catania, N. Chauché, J. A. Dowdeswell, B. Dorschel, I. Fenty, K. Hogan, I. Howat, A. Hubbard, M. Jakobsson, T. M. Jordan, K. K. Kjeldsen, R. Millan, L. Mayer, J. Mouginot, B. P. Y. Noël, C. O'Cofaigh, S. Palmer, S. Rysgaard, H. Seroussi, M. J. Siegert, P. Slabon, F. Straneo, M. R. van den Broeke, W. Weinrebe, M. Wood, K. B. Zinglensen (2017) *BedMachine v3: Complete bed topography and ocean bathymetry mapping of Greenland from multibeam echo sounding combined with mass conservation*, *Geophysical Research Letters*, 44, 11,051–11,061. <https://doi.org/10.1002/2017GL074954>.

Neteler, M., M. Bowman, M. Landa, M. Metz (2012) *GRASS GIS: a multi-purpose Open Source GIS*, *Environmental Modelling & Software* 31, 124-130, doi: 10.1016/j.envsoft.2011.11.014.

Nukissiorfiit (2005) *Grønlands vandkraftressourcer – en oversigt*, August 2005.

Teutschbein, C. and J. Seibert (2012) *Bias correction of regional climate model simulations for hydrological climate-change impact studies: Review and evaluation of different methods*, *Journal of Hydrology* 456-457, pp.12-29.

Yue, S., P. Pilon, G. Cavadias (2002) *Power of the Mann-Kendall and Spearman's rho test for detecting monotonic trends in hydrological series*, *Journal of Hydrology*, Vol. 259, 254-271.